

# Compact UWB MIMO Vivaldi Antenna With Dual Band-Notched Characteristics

ZHENYA LI<sup>1,2</sup>, CHENGYOU YIN<sup>1</sup>, AND XIAOSONG ZHU<sup>1</sup>

<sup>1</sup>Institute of Electronic Countermeasure, National University of Defense Technology, Hefei 230037, China

<sup>2</sup>State Key Laboratory of Pulsed Power Laser Technology, National University of Defense Technology, Hefei 230037, China

Corresponding author: Zhenya Li (lizhenya7189@126.com)

This work was supported by the National Natural Science Foundation of China under Grant 61671453 and Grant 61671454.

**ABSTRACT** A novel ultra-wideband (UWB) multiple-input multiple-output (MIMO) Vivaldi antenna with dual band-notched characteristics is presented and fabricated. The antenna is comprised of an improved ground plane and two microstrip feeding lines with a compact size of  $26 \times 26 \text{ mm}^2$ . The evolutionary process of the antenna is given. By etching the T-shaped slot on the ground plane, the port isolation between individual antenna elements can be greatly increased. Meanwhile, by adding two split ring resonator (SRR) of different sizes next to the microstrip feed lines, dual notches can be achieved to filter the interfere of WLAN and X-band communication satellites. The notched mechanism is analyzed from the surface current distributions. The experimental results show that the impedance bandwidth of the designed MIMO antenna is from 2.9 to 11.6 GHz, along with two notched bands covering 5.3–5.8 GHz and 7.85–8.55 GHz, and the mutual coupling is less than  $-16 \text{ dB}$  in the whole working bandwidth. The MIMO antenna has good radiation characteristics, stable gain, and very low envelop correlation coefficient ( $\text{ECC} < 0.02$ ), which is suitable for UWB MIMO system applications. The idea in this paper also has a certain guiding significance for the study of band-notched MIMO Vivaldi antenna.

**INDEX TERMS** Band-notched, MIMO antenna, SRR, UWB, vivaldi antenna.

## I. INTRODUCTION

In the past few years, wireless communication systems has made great progress, and ultra-wideband(UWB) antenna has become more and more attractive [1]–[3]. Even though UWB technologies have significant advantages, such as low cost, high data rate and large communication capacity, they are also faced with the problems of reliability and multipath fading. To solve the problems, multiple-input multiple-output (MIMO) technology as a technical means has been proposed. Especially, it is important to combine UWB with MIMO technology, which can not only improve data transmission efficiency but also suppress the multipath effect. At the same time, it also can increase the communication quality and capacity.

There have been various UWB MIMO antennas to be presented [4]–[6]. It is necessary to ensure both small size and low mutual coupling for the MIMO antenna system. Under the condition that the antenna size is fixed, various different structures are used to isolate individual antenna elements for reducing the mutual coupling of MIMO antennas [7]–[13].

The associate editor coordinating the review of this manuscript and approving it for publication was Fang Yang.

In [7], a F-shaped stubs is reported to reduce the mutual coupling of MIMO antenna. A wideband neutralization line connecting two individual antenna is presented to reduce the mutual coupling in [8]. A UWB diversity antenna with CSRR structure to improve isolation is proposed in [9]. Several low mutual coupling MIMO antennas using different decoupling techniques are summarized [10]. The sizes of above MIMO antennas are still large, however it is particularly important to design miniaturized MIMO antennas. A ultra-compact high isolation UWB MIMO antenna is given [11]. A novel MIMO antenna using the technology of conceptual design and automated optimization is reported [12]. Planar MIMO antenna by the characteristic modes to improve isolation and achieve diversity pattern is studied [13]. Although a variety of UWB MIMO antennas with low mutual coupling are presented above, they still face the problem of narrowband interference.

As we all know, there are several existing narrowband communication systems within the designated UWB communication systems such as WiMAX (3.3–3.8GHz), WLAN (5.15–5.85GHz), and X-band communication satellites (7.9–8.4GHz) [14]–[16]. Therefore, it is desirable to design band-notched UWB MIMO antennas [17]–[24]. A UWB MIMO antenna with dual notched band and high isolation

is reported [17]. UWB MIMO antenna with notched band by differential feeding is studied [18]. To achieve the miniaturization of band-notched UWB MIMO antenna, Compact band-notched MIMO antenna is given for portable applications in [19]. A compact UWB MIMO antenna using koch fractal principle with band-notched characteristics is presented [20]. Compact band-notched UWB slot antenna for MIMO applications is proposed [21]. Ultra-compact band-notched MIMO antenna for UWB applications is studied [22]. Compact band-notched stepped-slot UWB-MIMO antenna by differential feeding with high isolation is reported [23]. A compact dual band-notched UWB diversity antenna with tapered feeding line is given [24]. Above studies on band-notched UWB MIMO antennas are mostly limited to UWB planar monopole or slot antennas, however it is necessary to study band-notched UWB MIMO vivaldi antennas. Vivaldi antenna, as an important UWB antenna, has the advantages of wide bandwidth, good directionality and low cross polarization, with the result that it is widely used in UWB systems. A stepped slot MIMO antenna for portable device applications with dual band-notched characteristics is studied [25], however, the notched performance needs to be improved. In [26], A compact tapered slot MIMO antenna with stepped slot to improve isolation is proposed, but it cannot filter out the narrow interference.

In this article, a novel UWB MIMO vivaldi antenna with dual band-notched characteristics is proposed. It has the size of only  $26 \times 26\text{mm}^2$ . By etching T-shaped slot in the ground plane, the port isolation between individual antenna elements can be greatly increased. The antenna can achieve dual band-notched characteristics by adding two split ring resonator(SRR) of different sizes next to the microstrip feed lines. Analyzed from the surface current distributions, the notched mechanism is given. The antenna is fabricated and measured. The experimental results are in good agreement with the simulated results.

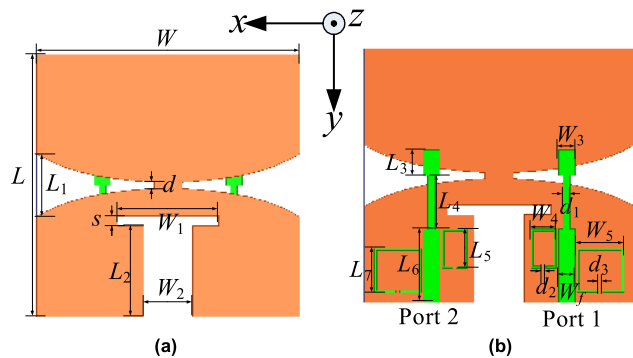


FIGURE 1. Configuration of the designed antenna. (a) Top view. (b) Bottom view.

## II. ANTENNA DESIGN AND ANALYSIS

### A. ANTENNA CONFIGURATIONS

The configuration of the designed dual band-notched UWB MIMO vivaldi antenna is shown in Fig.1. It is fabricated

on 0.762mm-thick Taconic RF-35 substrate. The dielectric constant  $\epsilon_r$  of it is 3.5 and the loss tangent is 0.0018. The overall dimensions of the MIMO antenna is  $26 \times 26\text{mm}^2$ . As shown in Fig. 1, the proposed antenna is fed by two  $50\Omega$  microstrip lines and consists of MIMO vivaldi antenna and four SRRs. The parameters of size are optimized and obtained by the Ansoft High Frequency Simulator Structure (HFSS). The Finally simulated values are as below(unit: mm):  $L = 26$ ,  $W = 26$ ,  $L_1 = 6.3$ ,  $W_1 = 10$ ,  $d = 0.6$ ,  $s = 1$ ,  $L_2 = 9$ ,  $W_2 = 4.8$ ,  $L_3 = 2.6$ ,  $L_4 = 5.5$ ,  $L_5 = 4$ ,  $L_6 = 7.5$ ,  $L_7 = 4.5$ ,  $W_3 = 1.6$ ,  $W_4 = 2.4$ ,  $W_5 = 4.5$ ,  $W_f = 1.6$ ,  $d_1 = 0.7$ ,  $d_2 = 0.4$ ,  $d_3 = 0.4$ . The tapered curve function of the vivaldi antenna is given as below :

$$y = C_1 \cdot e^{\alpha x} + C_2 \tag{1}$$

Here, the  $\alpha$  is 0.2.  $C_1$  and  $C_2$  can be determined by  $L_1$  and  $d$ .

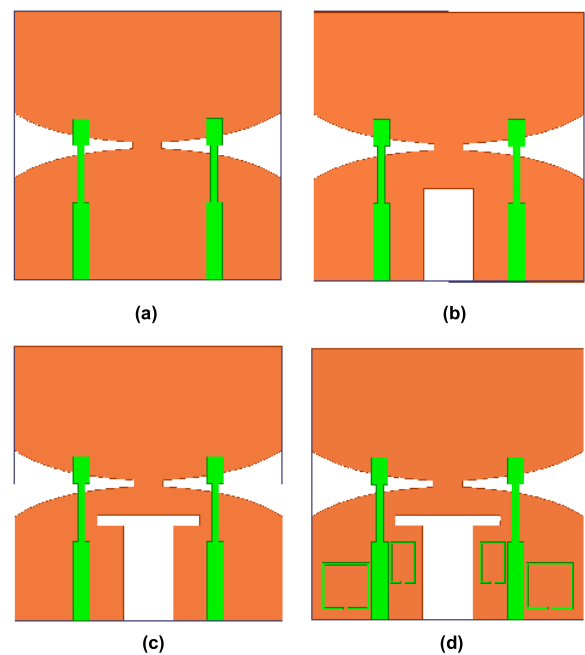


FIGURE 2. Evolutionary process of the designed MIMO antenna. (a) Antenna 1. (b) Antenna 2. (c) Antenna 3. (d) Antenna 4.

### B. DESIGN PROCESS

In order to better understand the design process of the antenna, four evolutionary iterations of the dual band-notched MIMO vivaldi antenna is shown in Fig. 2. Initially, a dual-port vivaldi antenna is depicted as shown in Antenna 1 of Fig. 2. Secondly, in order to decrease mutual coupling of the individual elements, a rectangular slot is etched on the ground plane, as shown in Antenna 2 of Fig. 2. Thirdly, to further increase the port isolation of the antenna elements, T-shaped slot is etched on the ground plane. T-shaped slot can reduce the surface current on the ground plane between two ports, thus reducing mutual coupling. Finally, to suppress the narrowband interference of WLAN and X-band communication satellite, two different SRRs are added near

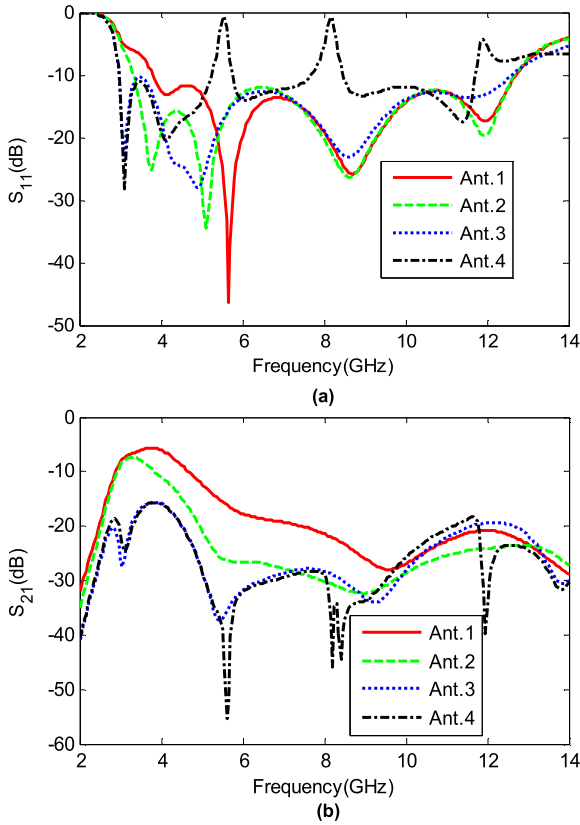


FIGURE 3. S-Parameters of the proposed antenna. (a)  $S_{11}$  (b)  $S_{21}$ .

each microstrip line. The length of larger SRR is 17.6mm and the length of smaller SRR is 12.4mm. By adding SRR, good notched characteristics can be achieved. The comparison of simulated S-Parameters of four evolutionary antennas is given in Fig. 3. Seen from Fig. 3, the simulated impedance bandwidth of original Antenna 1 is 3.8-12.7GHz. By etching T-shaped slot on the ground plane, the impedance of low frequencies can be improved with the impedance bandwidth increasing greatly, and the mutual coupling at low frequencies are reduced well. The impedance bandwidth of the finally designed antenna is 2.9-11.7GHz with two notched bands 5.2-5.8GHz and 7.8-8.5GHz. Therefore, the antenna can filter the narrowband interference well.

C. NOTCHED MECHANISM

Fig. 4 illustrates the surface current distributions of the designed antenna at two notched frequencies 5.5 and 8.2GHz, respectively. The antenna was excited by port 1, and port 2 was terminated with 50Ω loading. When the antenna operates at 5.5GHz, the larger SRR is equivalent to a resonator, which has a resonance effect on the antenna. Most of the surface current energy are concentrated on the SRR and the antenna almost cannot radiate outside. In the same way, When the antenna operates at 8.2GHz, Most of the surface current energy are concentrated on the smaller SRR and the antenna can achieve band-notched characteristics. So, by

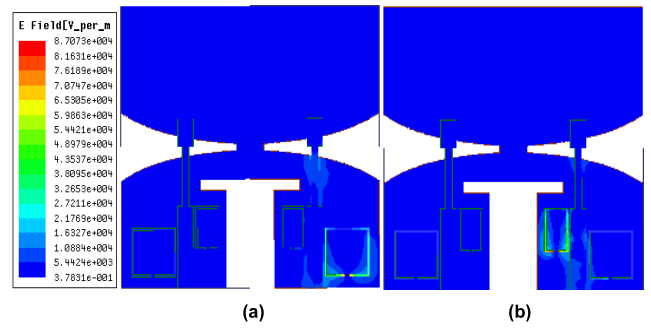


FIGURE 4. Surface current distributions of the MIMO antenna at two notched frequencies. (a) 5.5GHz (b) 8.2GHz.

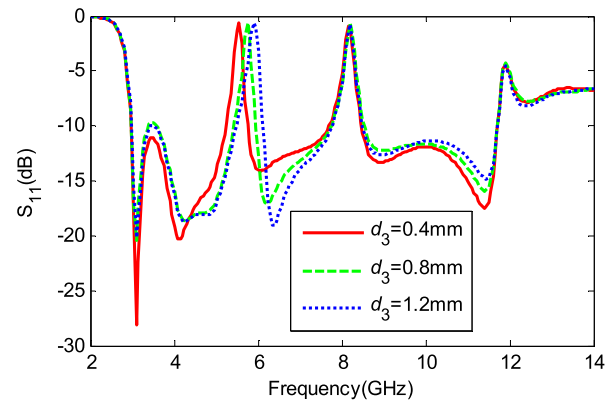


FIGURE 5. Variation curve of  $S_{11}$  with different  $d_3$ .

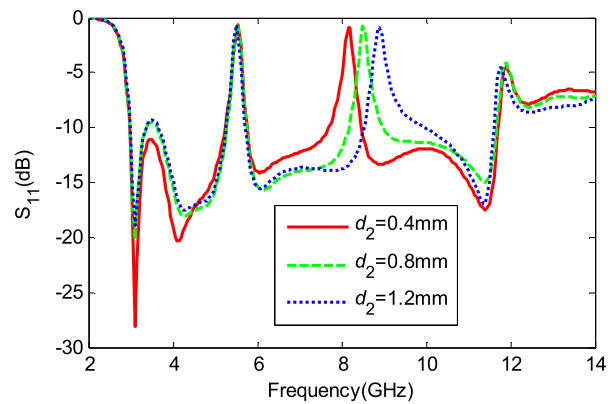


FIGURE 6. Variation curve of  $S_{11}$  with different  $d_2$ .

adding SRRs of different sizes next to the microstrip feed lines, the antenna can generate dual notched bands.

D. PARAMETRIC STUDY

The variation curve of  $S_{11}$  with different  $d_3$  is displayed in Fig. 5. It can be seen that as  $d_3$  increases, the notched central frequency at the low frequency increases gradually, while the notched central frequency at high frequency is basically unchanged. Fig. 6 shows the variation of  $S_{11}$  with different  $d_2$ . Similarly, as  $d_2$  increases, the notched central frequency at the high frequency increases gradually, while

the notched central frequency at the low frequency is basically unchanged. Therefore, it can be seen that the notched performance of the designed antenna are mainly determined by SRR. At the same time, the notched band of the designed antenna can be flexibly controlled by altering the opening slot width of SRR.

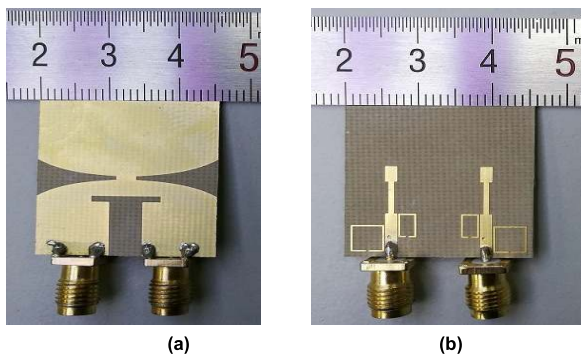


FIGURE 7. Fabricated photograph of the MIMO antenna. (a) Top view (b) Bottom view.

### III. RESULTS AND DISCUSSIONS

To ensure the practical value and the correctness of simulation, the proposed antenna is fabricated based on the above optimized size of antenna in section two. Fig.7 gives the fabricated photograph of the band-notched MIMO antenna. By using the vector network analyzer, we measured the S-Parameters of the antenna. To get more accurate results, the radiation pattern and gain performance of the antenna is tested in a microwave anechoic chamber.

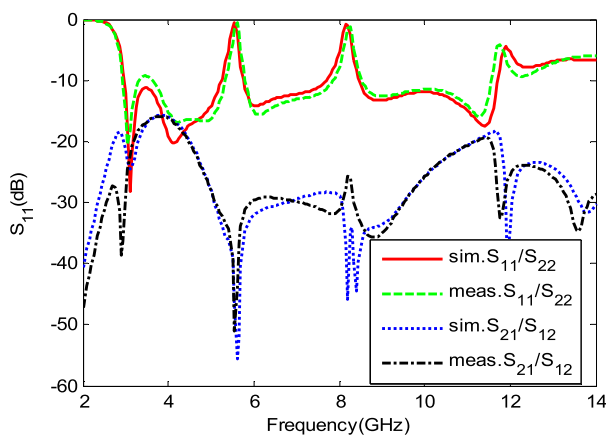


FIGURE 8. Measured S-Parameters of MIMO antenna.

#### A. RETURN LOSS

The experimental S-Parameters including  $S_{11}/S_{22}$  and  $S_{21}/S_{12}$  are shown in Fig. 8. Seen from Fig. 8, the measured S-Parameters agree well with the simulated results. The measured impedance bandwidth of the proposed antenna is from 2.9 to 11.6GHz with  $S_{11} < -10\text{dB}$ , along with two notched bands covering 5.3-5.8GHz and 7.85-8.55GHz.

The two notched bands respectively correspond to 5.5GHz WLAN and 8.2GHz communication satellites bands. The measured transmission coefficient ( $S_{12} = S_{21}$ ) is less than  $-16\text{dB}$  in the whole frequency band from 2 to 14GHz. The proposed MIMO antenna has good port isolation and the mutual coupling is relatively low.

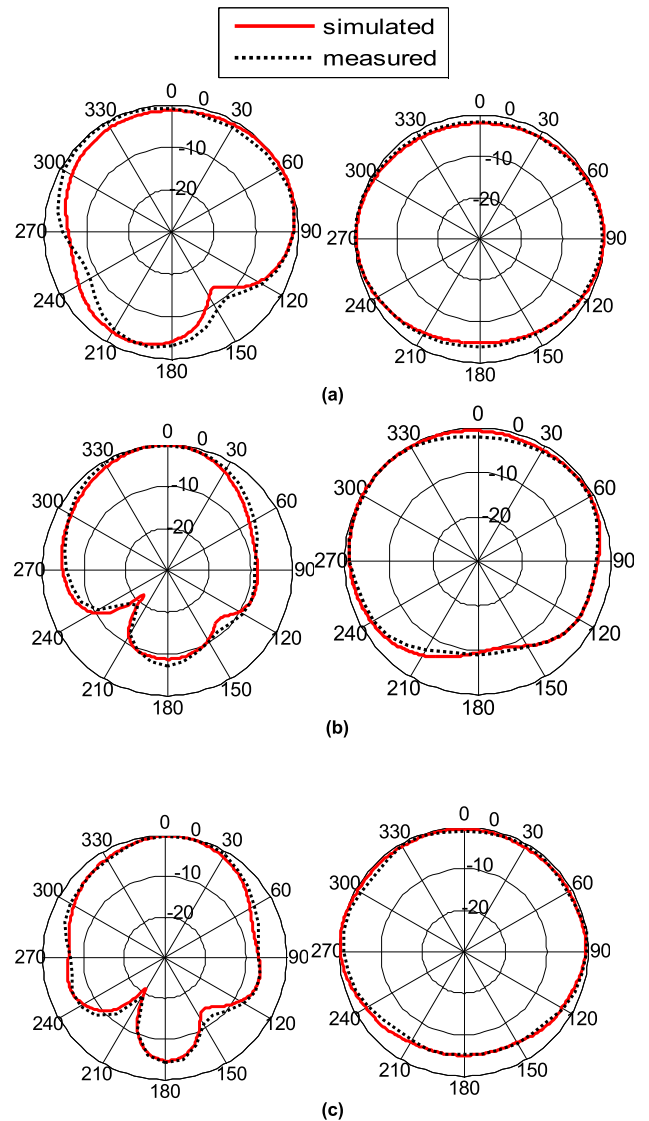


FIGURE 9. Measured radiation patterns of xoy plane(left) and xoz plane(right). (a) 4GHz (b) 7GHz (c) 9GHz.

#### B. RADIATION PATTERN AND GAIN

Fig. 9 shows the simulated and tested normalized radiation patterns of the presented MIMO antenna at 4, 7, and 9GHz, when port 1 was fed and port 2 was terminated with  $50\Omega$  loading. The consistency of the simulated and measured radiation patterns verifies the correctness of the design. The proposed antenna has end-fire characteristics.

Fig. 10 describes the gain of UWB and proposed band-notched MIMO antennas under the condition that port 1 was excited. Here, the UWB antenna refers to Antenna 3 above, without SRR ring. From the Fig. 10, we can see that



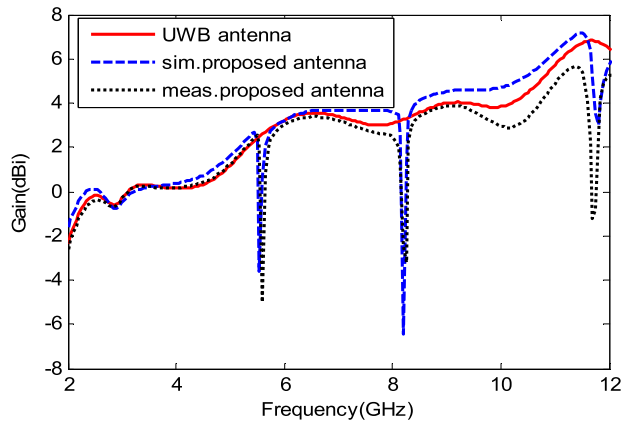


FIGURE 10. Measured gain of the MIMO vivaldi antenna.

the gain of UWB MIMO antenna is basically stable, however the gain of the designed band-notched MIMO antenna decreases sharply in notched band. The experimental results demonstrate the designed MIMO antenna is suitable for UWB communication applications with good band-notched characteristics.

C. DIVERSITY ANALYSIS

The diversity characteristics of MIMO antenna is an valuable features, and it can be evaluated from the envelope correlation coefficient(ECC). Usually in order to obtain better antenna performance, the ECC must be very small. The ECC can be calculated by S-Parameters according to the below formula [27].

$$ECC = \frac{|S_{11}^* S_{12} + S_{21}^* S_{22}|^2}{(1 - |S_{11}|^2 - |S_{21}|^2)(1 - |S_{22}|^2 - |S_{12}|^2)} \quad (2)$$

The experimental ECC is illustrated in Fig.11. It is seen that the ECC is very small and less than 0.02 within the entire impedance bandwidth, which indicates the MIMO antenna has good diversity characteristics.

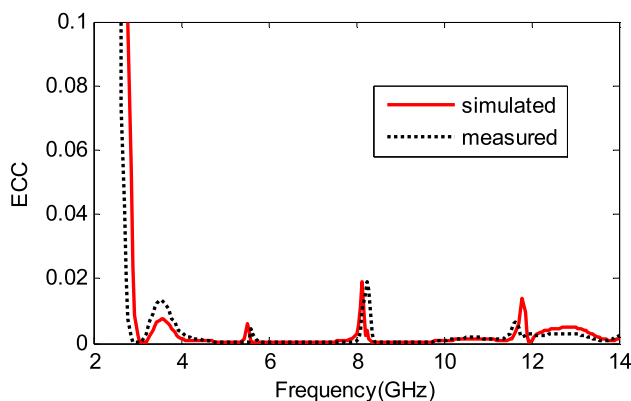


FIGURE 11. ECC of the designed MIMO antenna.

IV. CONCLUSION

A novel UWB MIMO vivaldi antenna with dual band-notched characteristics is presented and fabricated. It has the compact

size of 26 × 26mm<sup>2</sup>. The evolutionary process of the antenna is given and the variation of notched characteristics with SRR parameters is studied. Moreover, the notched mechanism is analyzed from the surface current distributions. Good agreement is displayed between the simulated and experimental results. The experimental impedance bandwidth of the MIMO vivaldi antenna is 2.9-11.6GHz, along with two notched bands covering 5.3-5.8GHz and 7.85-8.55GHz. The tested mutual coupling is less than -16dB in the whole operating band. Besides, the antenna has good radiating characteristics, stable gain, and very low ECC, which is suitable for UWB communication and MIMO system applications.

REFERENCES

- [1] N. Chahat, M. Zhadobov, R. Sauleau, and K. Ito, "A compact UWB antenna for on-body applications," *IEEE Trans. Antennas Propag.*, vol. 59, no. 4, pp. 1123-1131, Apr. 2011.
- [2] M.-C. Tang, T. Shi, and R. W. Ziolkowski, "Planar ultrawideband antennas with improved realized gain performance," *IEEE Trans. Antenna Propag.*, vol. 64, no. 1, pp. 61-69, Jan. 2016.
- [3] Z. Li, X. Zhu, and C. Yin, "CPW-fed ultra-wideband slot antenna with broadband dual circular polarization," *AEU-Int. J. Electron. Commun.*, vol. 98, pp. 191-198, Jan. 2019.
- [4] L. Liu, S. W. Cheung, and T. I. Yuk, "Compact MIMO antenna for portable devices in UWB applications," *IEEE Trans. Antennas Propag.*, vol. 61, no. 8, pp. 4257-4264, Aug. 2013.
- [5] J.-Y. Zhang, F. Zhang, W.-P. Tian, and Y.-L. Luo, "ACS-fed UWB-MIMO antenna with shared radiator," *Electron. Lett.*, vol. 51, no. 17, pp. 1301-1302, Sep. 2015.
- [6] R. Hussain, M. S. Sharawi, and A. Shamim, "An integrated four-element slot-based MIMO and a UWB sensing antenna system for CR platforms," *IEEE Trans. Antennas Propag.*, vol. 66, no. 2, pp. 978-983, Feb. 2018.
- [7] A. Iqbal, O. A. Saraereh, A. W. Ahmad, and S. Bashir, "MMutual coupling reduction using F-shaped stubs in UWB-MIMO antenna," *IEEE Access*, vol. 6, pp. 2755-2759, 2018.
- [8] S. Zhang and G. F. Pedersen, "Mutual coupling reduction for UWB MIMO antennas with a wideband neutralization line," *IEEE Antennas Wireless Propag. Lett.*, vol. 15, pp. 166-169, 2016.
- [9] M. S. Khan, A.-D. Capobianco, S. M. Asif, D. E. Anagnostou, R. M. Shubair, and B. D. Braaten, "A compact CSRR-enabled UWB diversity antenna," *IEEE Antennas Wireless Propag. Lett.*, vol. 16, pp. 808-812, 2017.
- [10] I. Nadeem and D.-U. Choi, "Study on mutual coupling reduction technique for MIMO antennas," *IEEE Access*, vol. 7, pp. 563-586, 2019.
- [11] M. S. Khan, A. D. Capobianco, A. Iftikhar, R. M. Shubair, D. E. Anagnostou, and B. D. Braaten, "Ultra-compact dual-polarised UWB MIMO antenna with meandered feeding lines," *IET Microw. Antennas Propag.*, vol. 11, no. 7, pp. 997-1002, 2017.
- [12] S. Kozziel, A. Bekasiewicz, and Q. S. Cheng, "Conceptual design and automated optimisation of a novel compact UWB MIMO slot antenna," *IET Microw., Antennas Propag.*, vol. 11, no. 8, pp. 1162-1168, 2017.
- [13] X. Zhao, S. P. Yeo, and L. C. Ong, "Planar UWB MIMO antenna with pattern diversity and isolation improvement for mobile platform based on the theory of characteristic modes," *IEEE Trans. Antennas Propag.*, vol. 66, no. 1, pp. 420-425, Jan. 2018.
- [14] H. Hosseini, H. R. Hassani, and M. H. Amini, "Miniaturised multiple notched omnidirectional UWB monopole antenna," *Electron. Lett.*, vol. 54, no. 8, pp. 472-474, 2018.
- [15] I. B. Vendik, A. Rusakov, K. Kanjanasit, J. S. Hong, and D. Filonov, "Ultrawideband (UWB) planar antenna with single-, dual-, and triple-band notched characteristic based on electric ring resonator," *IEEE Antennas Wireless Propag. Lett.*, vol. 16, pp. 1597-1600, 2017.
- [16] S. Doddipalli and A. Kothari, "Compact UWB antenna with integrated triple notch bands for WBAN application," *IEEE Access*, vol. 7, pp. 183-190, 2019.
- [17] J.-F. Li, Q.-X. Chu, Z.-H. Li, and X.-X. Xia, "Compact dual band-notched UWB MIMO antenna with high isolation," *IEEE Trans. Antennas Propag.*, vol. 61, no. 9, pp. 4759-4766, Sep. 2013.

- [18] H. Huang, Y. Liu, and S. Gong, "Uniplanar differentially driven UWB polarisation diversity antenna with band-notched characteristics," *Electron. Lett.*, vol. 51, no. 3, pp. 206–207, 2015.
- [19] L. Liu, S. W. Cheung, and T. I. Yuk, "Compact MIMO antenna for portable UWB applications with band-notched characteristic," *IEEE Trans. Antennas Propag.*, vol. 63, no. 5, pp. 1917–1924, May 2015.
- [20] S. Tripathi, A. Mohan, and S. Yadav, "A compact koch fractal UWB MIMO antenna with WLAN band-rejection," *IEEE Antennas Wireless Propag. Lett.*, vol. 14, pp. 1565–1568, 2015.
- [21] R. Chandel and A. K. Gautam, "Compact MIMO/diversity slot antenna for UWB applications with band-notched characteristic," *Electron. Lett.*, vol. 52, no. 5, pp. 336–338, 2016.
- [22] A. K. Gautam, S. Yadav, and K. Rambabu, "Design of ultra-compact UWB antenna with band-notched characteristics for MIMO applications," *IET Microw., Antennas Propag.*, vol. 12, no. 12, pp. 1895–1900, 2018.
- [23] Y.-Y. Liu and Z.-H. Tu, "Compact differential band-notched stepped-slot UWB-MIMO antenna with common-mode suppression," *IEEE Antennas Wireless Propag. Lett.*, vol. 16, pp. 593–596, 2017.
- [24] R. Chandel, A. K. Gautam, and K. Rambabu, "Tapered fed compact UWB MIMO-diversity antenna with dual band-notched characteristics," *IEEE Trans. Antennas Propag.*, vol. 66, no. 4, pp. 1677–1684, Apr. 2018.
- [25] C. R. Jetti and V. R. Nandanavanam, "Trident-shape strip loaded dual band-notched UWB MIMO antenna for portable device applications," *Int. J. Electron. Commun.*, vol. 83, pp. 11–21, Jan. 2018.
- [26] H.-F. Huang and Z.-P. Zhang, "Mutual coupling reduction of a very compact UWB-MIMO linearly tapered slot antenna using a simple stepped slot," in *Proc. IEEE Int. Appl. Comput. Electromagn. Soc. Symp. (ACES)*, Aug. 2017, pp. 1–2.
- [27] S. Blanch, J. Romeu, and I. Corbella, "Exact representation of antenna system diversity performance from input parameter description," *Electron. Lett.*, vol. 39, no. 9, pp. 705–707, May 2003.



**ZHENYA LI** was born in Anyang, Henan, China, in 1989. He received the B.S. and M.S. degrees from the Hefei Electronic Engineering Institute (HEEI), in 2012 and 2015, respectively. He is currently pursuing the Ph.D. degree with the Institute of Electronic Countermeasure, National University of Defense Technology (NUDT). His research interests include ultra-wideband antenna, CP antenna, conformal antenna, and antenna array designs.



**CHENGYOU YIN** was born in Chaohu, Anhui, China, in 1964. He received the B.S. degree from the Hefei Electronic Engineering Institute (HEEI), in 1985, the M.S. degree from Xidian University, in 1988, and the Ph.D. degree from the University of Science and Technology of China (USTC), in 1998, all in electronic engineering. He is currently a Professor with the National University of Defense Technology (NUDT). His research interests include radar signal processing, microwave techniques, numerical methods in electromagnetic, array signal processing, and data fusion.



**XIAOSONG ZHU** was born in Hefei, Anhui, China, in 1963. He received the B.S. degree in radio technology from Anhui University, in 1984, and the M.S. degree in circuit and system from the University of Electronic Science and Technology of China, in 1990. He is currently a Professor with the National University of Defense Technology (NUDT). His research interests include RF circuit, mobile communication systems, smart signal processing, and smart skin technology.

...